Deletion of *Drosophila* insulin-like peptides causes growth defects and metabolic abnormalities

Hua Zhang[a,1], Jingnan Liu[a,1], Caroline R. Li[b], Bahram Momen[c], Ronald A. Kohanski[d], and Leslie Pick[a,b,2]

[a]Department of Entomology, [b]Program in Molecular and Cell Biology, and [c]Department of Environmental Science and Technology, University of Maryland, College Park, MD 20742; and [d]Departments of Pediatrics and Pharmacology, Johns Hopkins Medical Institutes, Baltimore, MD 21205

Edited by M. Daniel Lane, Johns Hopkins University School of Medicine, Baltimore, MD, and approved September 29, 2009 (received for review May 11, 2009)

Insulin/Insulin-like growth factor signaling regulates homeostasis and growth in mammals, and is implicated in diseases from diabetes to cancer. In *Drosophila melanogaster*, as in other invertebrates, multiple Insulin-Like Peptides (DILPs) are encoded by a family of related genes. To assess DILPs' physiological roles, we generated small deficiencies that uncover single or multiple *dilps*, generating genetic loss-of-function mutations. Deletion of *dilps1–5* generated homozygotes that are small, severely growth-delayed, and poorly viable and fertile. These animals display reduced metabolic activity, decreased triglyceride levels and prematurely activate autophagy, indicative of "starvation in the midst of plenty," a hallmark of Type I diabetes. Furthermore, circulating sugar levels are elevated in *Df[dilp1–5]* homozygotes during eating and fasting. In contrast, *Df[dilp6]* or *Df[dilp7]* animals showed no major metabolic defects. We discuss physiological differences between mammals and insects that may explain the unexpected survival of lean, 'diabetic' flies.

diabetes | DILP | *Drosophila* insulin receptor | insect physiology | trehalose

Drosophila melanogaster is an excellent model for studying the molecular bases of human disease because of the high degree of conservation of fundamental biological processes throughout the animal kingdom. Abnormalities in Insulin/Insulin-like growth factor-1 Signaling (IIS) have been implicated in a broad range of diseases from diabetes and obesity, to cancer (1–4). In Type 1 diabetes mellitus, autoimmune destruction of pancreatic β-cells results in decreased insulin production. Circulating sugar levels then rise due to failure of glucose uptake by insulin-dependent glucose transport, exacerbated by increased gluconeogenesis in tissues where low sugar levels trigger starvation responses and the breakdown of glycogen and fat to produce energy. Thus, this disease has been referred to as "starvation in the midst of plenty," as the body fails to use energy from ingested food sources, and initiates compensatory starvation responses [reviewed in (2)]. Much has been learned about the molecular basis of IIS-associated disease from mouse models [reviewed in (4–7)]. In keeping with clinical expectations, loss-of-function mutations in murine insulin and insulin receptor genes resulted in severe diabetes, with death of newborn mice occurring within days of birth (8, 9). Similarly, the roles of IGF-1 and IGF-1 receptor in promoting growth were supported by the finding that loss-of-function mutants were severely growth-impaired (10). These studies also revealed redundancy and crosstalk in the system (3, 11, 12), which, together with epidemiological and genome-wide association studies in humans, highlight the fact that diabetes, obesity, and insulin resistance are complex, multifactorial diseases [reviewed in (13, 14)]. These complexities support the notion that simple model systems, such as *Drosophila* will be useful for understanding the basis of IIS-associated diseases.

Drosophila harbor a single IIS-family receptor, the *Drosophila* insulin receptor (DInR), identified in O. Rosen's lab in the 1980s (15, 16). Seven genes encoding candidate DInR ligands [*Drosophila* insulin-like peptides (DILPs)] with sequence and motif similarity to mammalian insulin were found in the *Drosophila* genome (17) (for an excellent comprehensive review, see 18). DILPs1–5 were predicted to be most closely related to mammalian insulin, while DILP6 and DILP7 were predicted to be more similar to IGF-1 and relaxin, respectively (17, 19). These seven *dilps* are expressed in diverse spatiotemporal patterns during development, suggesting differential functions (17). Other invertebrates also express a large number of insulin-like peptides (ILPs); for example, 38 putative *ilp* genes were found in the genome of *C. elegans*. It was suggested that these ligands have disparate functions by virtue of their differential spatiotemporal expression patterns. In addition, while insulins are canonical activators of Receptor Tyrosine Kinase (RTK) activity, some ligands in *C. elegans* may act as antagonists of IIS [reviewed in (20)]. For mosquitoes, eight ILPs have been identified (21) and functional studies indicate roles for different ILPs in egg laying, diapause, immunity, and metabolism (22–24). The ILPS are thought to be secreted proteins (25, 26), as are mammalian insulin and IGFs (2). In *Drosophila*, several lines of evidence suggest that DILPs are indeed DInR ligands: conditioned medium from cells expressing DILP2 or DILP5 activated DInR autophosphorylation (26) and overexpression of DILPs induced overgrowth, with increase in cell size and cell number, similar to overexpression of DInR (17, 27). Genetic interaction studies showed that large deficiencies uncovering *dilps1–5* suppressed DInR-mediated eye overgrowth phenotypes and, heterozygosity for *dinr* partially suppressed DILP2-mediated overgrowth (17). Four *dilps* (*1*,*2*,*3*,*5*) are expressed in clusters of median neurosecretory cells (mNSCs, also called Insulin Producing Cells, IPCs) of the brain (25–27), where levels of *dilp3* and *dilp5* RNA are nutrient-responsive (27). These cells appear to function like pancreatic β-cells, as IPC ablation resulted in elevated circulating sugar levels (26). In addition, IPC ablation resulted in increased longevity, developmental delay, and small animals (26, 28, 29), phenotypes similar to those seen for *chico* mutants and *dinr* transheterozygotes (30–32). The remaining *dilps* are expressed in different spatiotemporal patterns: *dilp4* is expressed in the embryonic mesoderm and anterior midgut, *dilp6* is expressed in the larval gut, and *dilp7* is expressed in specific cells in the larval and adult central nervous system (17, 19, 33).

Here, we used a genetic approach to study individual and redundant functions of the *dilp* gene family. We took advantage of the fact that *dilps1–5* are clustered on chromosome III to generate a small deficiency that simultaneously deletes all five genes. Animals lacking DILPs1–5 are homozygous viable and will reproduce but are small, poorly fertile, developmentally delayed, and display metabolic defects similar to those produced by loss of insulin function in mammals, including elevated sugar

PHYSIOLOGY

Author contributions: H.Z., B.M., and L.P. designed research; H.Z., J.L., and C.R.L. performed research; R.A.K. contributed new reagents/analytic tools; H.Z., J.L., C.R.L., B.M., and L.P. analyzed data; and L.P. wrote the paper.

The authors declare no conflict of interest.

This article is a PNAS Direct Submission.

[1]H.Z. and J.L. contributed equally to this paper

[2]To whom correspondence should be addressed. E-mail: lpick@umd.edu.

This article contains supporting information online at www.pnas.org/cgi/content/full/0905083106/DCSupplemental.

levels and initiation of starvation responses in fat tissue. The viability of these "diabetic" *Df[dilp1–5]* animals provides an in vivo system to investigate biochemical mechanisms underlying IIS-related metabolic defects with a long-term goal of screening for genetic and pharmacological inhibitors that ameliorate them.

Results

Small Deficiencies to Delete *dilps*. Our initial approach to study DILP loss-of-function was to generate individual RNAi lines to separately target each of the 7 *dilps*. None of these RNAi lines affected body growth or tissue size using a number of different *GAL4* drivers. One interpretation of the absence of growth defects is that there is functional redundancy among *dilps*. In keeping with this, a recent paper reported that expression of *dilp2* RNAi resulted in a compensatory increase in *dilp3* levels (34). With 7 *dilp* genes, it is virtually impossible to assess functional redundancy using combinations of individual RNAi lines, which may vary in their effectiveness overall or in different cell types. The likelihood that only partial knockdown will be achieved further complicates interpretation of results obtained with the RNAi approach. We therefore decided to get a first assessment of loss-of-function effects by generating small deficiencies that uncover *dilp* genes. Using the *FLP-FRT* system (35), we generated three deficiencies: *Df[dilp1–5]*, *Df [dilp6]*, and *Df[dilp7]*. The sizes of the deletions are approximately 60.5, 15.7, and 22.9 kb, respectively (Fig. S1). As *dilp6* and *dilp7* are both on the X chromosome, recombination was used to generate *Df[dilp6, 7]*. In addition to the *dilp*s, several genes are also completely or partially deleted in these deficiency lines. Of these genes, the only one known to be required for viability is *CG2864*, which is removed in *Df[dilp7]* and encodes Poly(ADP-ribose)glycohydrolase (*Parg*, 36).

***Df[dilp1–5]* Homozygotes Are Viable and Fertile, but Growth Impaired.** All deficiency lines were isolated and maintained over balancer chromosomes. In the stock of *Df[dilp1–5]/TM6bTb*, a small number of *non-Tb* larvae were observed. These animals were transferred to fresh vials, and were found to eclose to adults and breed. These *Df[dilp1–5]* homozygotes competed poorly with wild-type or heterozygous flies, but, with careful attention, could be maintained as a viable and fertile stock on standard medium and at varying temperatures. To confirm that these animals were indeed *Df[dilp1–5]* homozygotes, and not a result of a rare recombination, PCR was used to verify the absence of the coding regions for *dilps1,2,3,4*, and *5* and to confirm the expected deletion junctions (Figs. S1 and S2).

Df[dilp1–5] homozygous adults were small (Fig. 1*A*) with decreased body mass (Fig. 1*B*) and were developmentally delayed. The developmental time to reach the wandering third-instar stage was lengthened to more than 9 days, compared to 5 days for controls, and the time to reach pupation was also extended, but the time from pupation to eclosion was not greatly affected. These small size and developmental delay phenotypes resemble those seen for surviving *dinr* transheterozygotes (30, 31). None of these phenotypic defects were observed in *Df[dilp1–5]* heterozygotes. The phenotypes observed in *Df[dilp1–5]* homozygotes are not likely due to the absence of additional genes removed in the deficiency: *CG8177* and *CG33205* are disrupted in the parental lines used to generate *Df[dilp1–5]* and these do not show growth defects. For *CG14168* and *CG32052*, P-element insertion lines were obtained and homozygotes were similar in size to wild-type controls. Finally, expression of DILP2 in these animals, using *hsGAL4*>*UASdilp2*, was sufficient to rescue growth defects: the size of *Df[dilp1–5]* homozygotes expressing DILP2 was comparable to wild-type (Fig. 1 *D* and *E*). Developmental delay was largely rescued as well, with homozygotes reaching the wandering third-instar larval stage after 6 days.

Fig. 1. Deletion of *dilps1–5* impairs organismal growth. (*A*) *Df[dilp1–5]* adult homozygotes are viable but small. Photos of adults 1 day after eclosion: (left) w^{1118}; (right) *Df[dilp1–5]/Df[dilp1–5]*. (*B* and *C*) Body weight of virgin females (*B*) or unmated males (*C*) of control and *dilp* deficiencies, as indicated. Data represents mean ± standard error. The body size and weight of *Df[dilp1–5]* was reduced. (*D* and *E*) *Df[dilp1–5]* larvae and pupae are small. Photos of third-instar larvae (*D*) or pupae (*E*) are shown; (left), parental control line d02657; (middle), *Df[dilp1–5]* homozygotes; (right), 'rescued' *Df[dilp1–5]* homozygotes (*hsGAL4*>*UASdilp2*; *Df[dilp1–5]/Df[dilp1–5]*). Growth defects in *Df[dilp1–5]* homozygotes were fully rescued by low level ubiquitous expression of DILP2 at 25 °C.

To determine the basis of the small size of *Df[dilp1–5]* homozygotes, wings were dissected and cell size and cell number were determined, as described (17). Examination of wings revealed smaller overall size and area (Fig. 2*A–C*). This decrease reflected a decrease in cell number (Fig. 2*D*), as well as cell size (Fig. 2*E*). These phenotypes are similar to those seen in *chico* mutants (32). Effects on cell size were further examined in the fat body, the major locus of fat storage in flies. Fat body cell size of *Df[dilp1–5]* homozygotes (Fig. 2 *G* and *J*) was 79% of the parental control line d02657 (Fig. 2 *F* and *I*) used to generate *Df[dilp1–5]*. This decrease in cell size was rescued by ubiquitous expression of DILP2 (Fig. 2 *H–L*). In sum, the reduced body size and developmental delay seen in the *Df[dilp1–5]* animals are consistent with roles for DILPs1,2,3,4, and/or 5 in the promotion and coordination of whole animal growth.

Df[dilp1–5] homozygotes displayed reduced fertility (Fig. S3). Although their egg laying displayed a similar time course to control females (Fig. S3*A* shows one sample experiment), their total lifetime egg production, and mean and maximal number of eggs laid per day were dramatically decreased (approximately 10% of the level of control animals; Fig. S3 *B* and *C*). Viability was also decreased; *Df[dilp1–5]* development to the pupal stage was decreased to approximately 45% of that of control animals and development to adult stages decreased to approximately 41% of that of control animals (Fig. S3*D*). Thus, it appears that both fertility and viability require DILP function but development from pupae to adults is less severely impacted by loss of

Fig. 2. Small size of *Df[dilp1–5]* homozygotes is due to reduced cell size and cell number. (*A–E*) Cell number and cell size in dissected wings. (*A* and *B*) Photos of dissected wings from (*A*) adult female, w^{1118} control or (*B*) *Df[dilp1–5]* homozygote. (*C*) The overall wing area is smaller in *Df[dilp1–5]* homozygotes than in w^{1118} controls. (*D* and *E*) Measurements of cell number and cell size in w^{1118} or *Df[dilp1–5]* homozygotes. Both decreased in *Df[dilp1–5]* mutants. $n = 5$ for *C–E*. (*F–K*) Fat body cell size is reduced in *Df[dilp1–5]* animals. Photos of larval fat bodies from wandering third-instar larvae stained with phalloidin (red) and DAPI (blue) to reveal nuclei. [×20 (*F*, *G*, and *H*); ×40 (*I*, *J*, and *K*).] Genotypes: (*F* and *I*) Control parental line d02657, (*G* and *J*) *Df[dilp1–5]/Df[dilp1–5]*, (*H*,*K*) *hsGAL4>UASdilp2*; *Df[dilp1–5]/Df[dilp1–5]*. (*L*) Quantitation of fat body cell size was carried out with ImageJ software. The cell size of *Df[dilp1–5]* homozygotes was approximately 80% of the parental control. Error bars indicate standard error.

DILP1–5 function than is fertility and development of eggs to pupal stages.

Allometry Is Disrupted in *Df[dilp1–5]* Homozygotes. It was reported that IIS plays a role in allometry, the relative proportioning of body parts (37, 38). Shingleton et al. (2005) showed that while most body organs scale down proportionately with small whole body size in *dinr* transheterozygotes, the male genitals do not scale proportionately. Similar effects were observed in *chico* mutant clones (37, 38). To test the role of DILPs in allometry, we compared the scaling of wings and male genital arches in *Df[dilp1–5]* homozygotes and d02657 parental controls. In *Df[dilp1–5]* homozygotes, male genital arch posterior lobes failed to scale proportionately with the smaller body and smaller wing size (Fig. 3). Wing size of *Df[dilp1–5]* homozygotes was reduced approximately 29% compared to parental controls. In contrast, genital arch posterior lobes, although still smaller than controls, were proportionately larger, reduced only approximately 15% compared to controls, a number very similar to the

Fig. 3. Loss of DILPs1–5 disproportionately affects body organ size. Mean area of (*A*) wings and (*B*) genital arch posterior lobes from adult males of the control parental line d02657 or *Df[dilp1–5]* homozygotes. Photos of (*C* and *D*) wings and (*E* and *F*) genital arch posterior lobes. Scale bars in panels (*C* and *E*) highlight the differences in organ size. Wing size in *Df[dilp1–5]* homozygotes is approximately 70% that of controls, while genital arches are smaller, but do not scale down proportionately. Data represents mean ± standard error.

16% reduction reported for *dinr* and *chico* (37). These results suggest that DILPs1,2,3,4, and/or 5 lie upstream of DInR and Chico to regulate cell growth and provide additional support for the hypothesis that different body organs respond differentially to IIS in *Drosophila*.

DILPs 6 and 7 Are Not Required for Viability. In contrast to *Df[dilp1–5]*, *Df[dilp6]* homozygotes were readily recovered (Figs. S1 and S2). These animals appeared fully viable and fertile. *Df[dilp6]* homozygotes did not display alterations in developmental rate, and body size was only mildly reduced (≈6% reduction compared to controls) (Fig. 1*B*). Other than this, no defects were apparent in *Df[dilp6]* homozygotes, which can be perpetuated as a healthy, true-breeding stock. *Df[dilp7]* homozygotes survived through larval stages but died after pupation. Occasionally, some *Df[dilp7]/Y* hemizygous male adult escapers were present. These escapers showed no discernible changes in body mass or size (Fig. 1*C*). The lethality associated with *Df[dilp7]* was rescued by ubiquitous expression of a *Poly(ADP-ribose) glycohydrolase* (*Parg*) transgene (*armGAL4>UAS-Parg*) (36), demonstrating that lethality was not caused by the absence of *dilp7*, but rather was due to the absence of the neighboring *Parg* gene that is removed along with *dilp7* in the deficiency (Fig. S1). However, the *Parg*-rescued *Df[dilp7]* animals (*Df[dilp7]*;*arm-GAL4*;*UAS-Parg*) were poorly fertile and it was not possible to generate a true-breeding stock for *Df[dilp7]*. This may be explained by the recent report that DILP7 is required for egg-laying (19). As *dilp6* and *7* are both on the X chromosome, recombination was used to generate *Df [dilp6,7]*. *Df[dilp6,7]* animals showed the same phenotypes as *Df[dilp7]*.

***Df[dilp1–5]* Homozygotes Exhibit Starvation Responses.** The storage of fat in insects is primarily in the form of triglycerides (39). Compared with wild-type controls, *Df[dilp1–5]* homozygotes showed a decrease in normalized whole body triglyceride levels (Fig. 4*A*), while *Df[dilp6]* homozygotes did not show any significant change.

In human Type I diabetics, the absence of insulin compromises the body's ability to use glucose and the body exhibits starvation responses, resulting in the breakdown of fat to provide energy. The *Drosophila* larva provides an excellent system to ask whether similar responses also occur in flies when insulin-like peptides are absent. Early third-instar larvae spend virtually all of their time eating, storing energy for impending metamorphosis. Following this eating period, larvae crawl out of the food, fasting for several hours before initiating pupation. At this time, autophagy

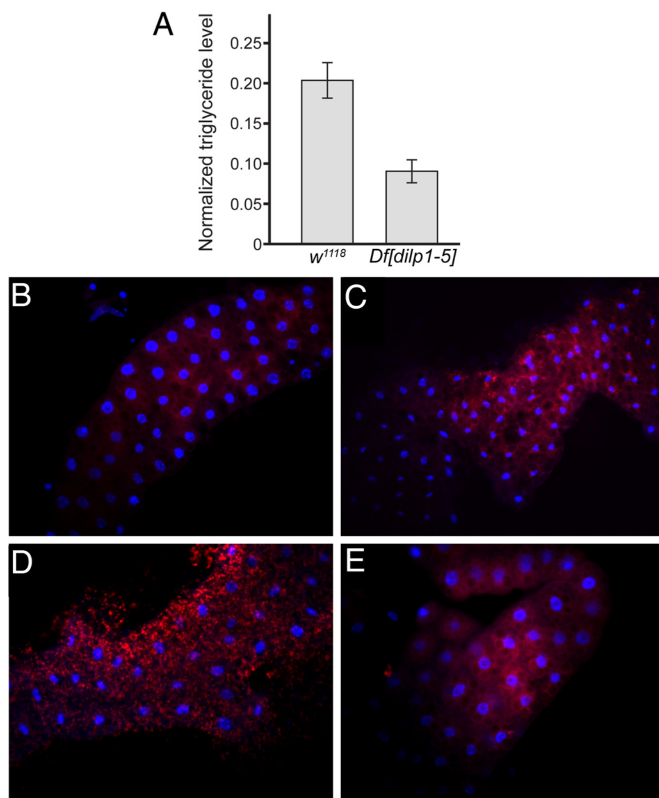

Fig. 4. *Df[dilp1–5]* homozygotes induce starvation responses. (*A*) Total body triglyceride level and total body protein from w^{1118} or *Df[dilp1–5]* adult male flies were measured; data shows the triglyceride levels normalized to the total protein level. Levels in *Df[dilp1–5]* animals were lower than the control. Normalized levels: w^{1118}, 0.204 ± 0.022, $n = 3$; *Df[dilp1–5]*, 0.090 ± 0.014, $n = 3$. Error bars indicate standard error. (*B–E*) *Df[dilp1–5]* homozygotes induce fat body autophagy, while actively eating. Lysotracker staining (red) of dissected fat bodies from third-instar larvae. Hoechst 33342 (blue) reveals nuclei. For (*B*, *C*, and *E*), larvae were actively eating, burrowed in the food and had full guts. Genotypes: (*B*) Control parental line d02657; (*C*) *Df[dilp1–5]/Df[dilp1–5]*; (*D*) Control parental line d02657; burrowed third-instar larva removed from food and starved for 3 h in the presence of water (*E*) *hsGAL4*>*UASdilp2*; *Df[dilp1–5]/Df[dilp1–5]*. Feeding *Df[dilp1–5]* homozygotes (*C*) resembled starved control animals (*D*).

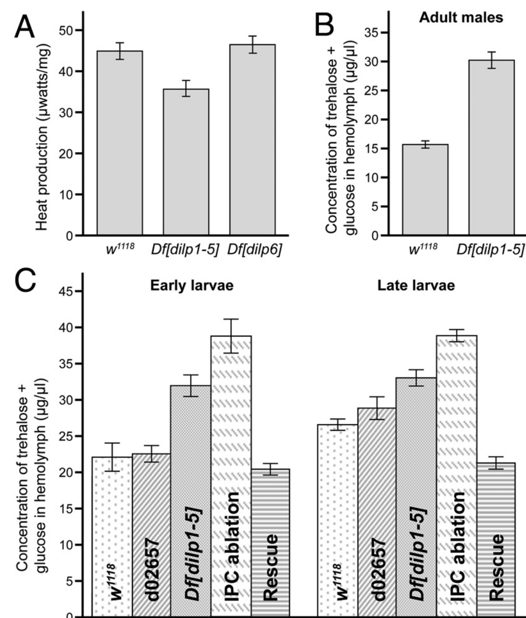

Fig. 5. Diabetic-like manifestations of *Df[dilp1–5]* homozygotes. (*A*) *Df[dilp1–5]* homozygotes show decreased metabolic rates. The overall metabolic rates of w^{1118}, *Df[dilp1–5]* or *Df[dilp6]* third-instar larvae, as indicated, were measured as the resting heat production normalized to body dry mass. Heat production rates were: w^{1118}, 44.89 ± 2.02, $n = 18$; *Df[dilp1–5]*, 35.61 ± 2.14, $n = 16$; *Df[dilp6]*, 46.46 ± 2.08, $n = 17$. Data represents mean ± standard error. (*B* and *C*) Circulating sugar levels are elevated in *Df[dilp1–5]* homozygotes. Sugar levels (trehalose + glucose) were determined in hemolymph extracted from (*B*) adult males, 3–5 days after eclosion, ($n = 3$) or (*C*) early or late third-instar larvae, as indicated. Levels are indicated for negative controls: w^{1118} and parental line d02657; for experimental samples: *Df[dilp1–5]/Df[dilp1–5]*, and *hsGAL4*>*UASdilp2*; *Df[dilp1–5]/Df[dilp1–5]*; (Rescue) and for the positive control: *dilp2-GAL4*>*UAS-rpr* (IPC ablation). Larval hemolymph was collected from 10–15 animals and pooled for each genotype (*SI Experimental Procedures*); a minimum of five replicates was used for each bar shown in the graph. The circulating sugar levels of *Df[dilp1–5]* homozygotes were higher than controls in early and late third-instar larvae. Levels were lowered by ubiquitous expression of DILP2. Sugar levels were highest in animals in which IPCs had been ablated (*dilp2GAL4*>*UASrpr*). Error bars indicate standard error.

(destruction of cellular components to garner nutrients) is activated in the fat body (40, 41).

To test whether *Df[dilp1–5]* animals display starvation responses while actively eating, lysotracker was used to monitor activation of autophagy. In control feeding larvae, only basal levels of lysotracker staining were evident (Fig. 4*B*), but high levels of lysotracker positive staining were apparent in actively feeding *Df[dilp1–5]* larvae (Fig. 4*C*). This pattern of lysotracker staining resembled that seen in control animals that had been starved (Fig. 4*D*). Expression of DILP2 in *Df[dilp1–5]* larvae partially rescued this starvation response (Fig. 4*E*), implicating DILPs in the repression of autophagy, but also suggesting some DILPs may be more effective than others in signaling the fed state. Thus, *Df[dilp1–5]* homozygotes have decreased steady-state levels of stored triglycerides as adults and exhibit inappropriate breakdown of fat during larval feeding stages, reminiscent of responses normally associated with starvation.

***Df[dilp1–5]* Homozygotes Display Reduced Metabolic Activity.** Although *Df[dilp1–5]* homozygotes survived, they were less active than wild-type animals, and the mouth hook contraction rate appeared lower than that of controls. To assess whether this perceived sluggishness reflected a reduction in metabolic activity, the metabolic rates of wild-type larvae and larvae carrying *dilp* deficiencies were determined. The overall metabolic rate of *Df[dilp1–5]* homozygotes was reduced (Fig. 5*A*), consistent with these DILPs functioning in global homeostasis. In contrast, no significant difference in metabolic rate was observed between wild-type and *Df[dilp6]* larvae, demonstrating that *dilp6* is not required for global metabolic regulation in *Drosophila* larvae. The overall decrease in metabolic rate and lethargic behavior of *Df[dilp1–5]* homozygotes may reflect an inability of *Df[dilp1–5]* homozygotes to use nutrients.

Circulating Sugar Levels Are Elevated in *Df[dilp1–5]* Homozygotes. To test whether DILPs have an insulin-like function in regulating circulating sugar, we compared circulating sugar levels in the hemolymph of control and *Df[dilp1–5]* homozygous adults and larvae. In insects, the predominant circulating sugar is trehalose. Consistent with this, glucose comprised only approximately 2% of the total hemolymph sugar in our assays. In adult male *Df[dilp1–5]* homozygotes, hemolymph sugar levels were increased compared to control w^{1118} animals, suggesting that DILP function is required to regulate sugar homeostasis (Fig. 5*B*). To further investigate this, circulating sugar levels were measured in larvae of different genotypes (Fig. 5*C*). As *Df[dilp1–5]* homozygotes are developmentally delayed, it is important to control for

developmental stage. In fact, tests with wild-type animals revealed that circulating sugar levels were generally lower in early third-instar larvae than in late third-instar larvae. Thus, examining third-instar larvae without careful staging, or based solely upon timing, can obscure differences in sugar levels if one genotype or experimental group tends to develop more slowly than another. Based on this, circulating sugar levels in control and *Df[dilp1–5]* homozygous larvae were compared at two developmental stages: early third-instar larvae, when larval guts are full, and late third-instar larvae, when the guts have been cleared in preparation for pupation. At both developmental stages, circulating sugar levels were elevated in *Df[dilp1–5]* homozygotes (Fig. 5*C*, gray bar). This effect was rescued by expression of DILP2, which lowered circulating sugar to or even below wild-type levels (Fig. 5*C*, horizontally lined bar). In contrast to this, *Df[dilp6]* larvae showed no abnormalities in levels of circulating sugar. Interestingly, IPC ablated animals had even higher circulating sugar levels than *Df[dilp1–5]* homozygotes, suggesting that additional signals may be affected when these neurosecretory cells are ablated (Fig. 5*C*, hatched bar). In sum, *Df[dilp1–5]* homozygotes display elevated levels of circulating sugar, while actively eating and also during a period of developmentally-programmed fasting.

Discussion

Control of Growth and Metabolism by IIS Is Evolutionarily Conserved. IIS is highly conserved throughout the animal kingdom and is important for regulation of growth and metabolism in a range of organisms. In most cases, IIS receptors, IIS ligands, or both are represented by multigene families. In mice, where this has been examined in most detail, family members have both distinct and overlapping roles in regulating animal physiology [reviewed in (7, 42)]. Insulin-like activities were identified in invertebrates, including *Drosophila*, many years ago (43). Based upn genomic sequence and similarity to mammalian insulin, *Drosophila* have at least seven candidate IIS ligands. Evidence from RNAi experiments in our lab and published by others, while our work was in progress (34), indicate a high degree of redundancy among DILPs, including compensatory upregulation of expression of *dilp* gene(s), when others are experimentally downregulated. Thus, multiple approaches will be required to assess the functions of this complex multigene family. As a step toward defining DILP wild-type functions, we have taken a loss-of-function genetic approach that makes use of FRT sites in the *Drosophila* genome to generate small deficiencies that uncover genes of interest (35), followed by "adding back" a *dilp* gene to test for functional rescue. Many of the effects found to be associated with loss-of-DILP-function are reminiscent of defects in mammalian IIS [reviewed in (7, 13, 44)]. *Df[dilp1–5]* homozygotes exhibit growth defects (Figs. 1, 2, and 3), with decreases in overall body size due to decreases in cell size and cell number; developmental delay; and poor fertility and viability (Fig. S3). In keeping with DILPs functioning as DInR ligands, tissue-specific overexpression of DInR promotes growth (17) and some combinations of *dinr* alleles support survival but transheterozygotes are small and growth delayed (30, 31), similar to *Df[dilp1–5]* animals and *chico* mutants (32). Similar growth defects are observed in IGF-1 and IGF-1R null mice, which are developmentally delayed but viable [reviewed in (3)]. Interestingly, mouse IR and Ins null mutants are also small at birth, although larger than IGF-1/IGF-1R mutants. Similarly, several human syndromes point to a role for IR in growth regulation in humans: for example, Leprechaunism is associated with severe growth retardation and results from mutations in IR (45).

Metabolic control by IIS also shows many similarities between the *Drosophila* and mammalian systems. In mice, knock-out of the insulin receptor or the insulin genes resulted in diabetes, accompanied by hyperglycemia and ketoacidosis, resulting in perinatal lethality (3). These features phenocopy human Type I diabetes in which insulin production gradually fails. The *Df[dilp1–5]* homozygotes examined here show many defects similar to those in mammals: leanness, inappropriate breakdown of fat tissue, and high levels of circulating sugar (Figs. 4 and 5). These results demonstrate parallels in metabolic regulation between *Drosophila* and mammals. Furthermore, the counter-regulatory hormone to insulin, glucagon, appears to be functionally conserved in insects. Insect adipokinetic hormone (AKH) appears to act like mammalian glucagon by stimulating gluconeogenesis, as ablation of the corpora cardiaca cells that produce AKH caused decreased levels of sugar without affecting growth or developmental time (46).

Physiological Differences Between Insects and Mammals May Explain Survival of 'Diabetic' Flies. Unlike mammals with defective insulin or insulin genes, *Df[dilp1–5]* homozygotes survive and are fertile. At this point, we cannot rule out the possibility that compensatory action of DILP6 and/or DILP7 explains the survival of *Df[dilp1–5]* homozygotes, although neither *dilp6* nor *dilp7* mutant larvae showed metabolic defects. However, irrespective of this, it is clear that *Df[dilp1–5]* homozygotes do indeed display diabetic-like abnormalities, and it is thus surprising that they are not more severely affected. For example, even though these animals are breaking down fat, as evidenced by lower whole body triglycerides and activation of fat body autophagy, they do not appear to be suffering from acute effects of ketoacidosis that are toxic in mammals. Similarly, these animals appear relatively resistant to negative impacts of persistent hyperglycemia. This differential tolerance to long-term and endemic diabetic manifestations may reflect physiological differences between mammals and insects. First, the primary circulating sugar in insects is trehalose (47), a nonreducing disaccharide that will not generate glycation products, which are the cause of many of the long-term complications seen in human diabetes. Second, insects have endogenous mechanisms to raise sugar levels, and, in contrast to the situation for mammals where this increase is highly deleterious, this actually promotes the survival of insects under harsh conditions. For example, one of the mechanisms used by many insects to tolerate cold temperatures is the induction of high levels of polyols such as glycerol, or sugars, including trehalose, sorbitol, and others, that act as cryoprotectants [reviewed in (48, 49)]. The levels of these polyols and sugars vary over seasons, with levels increasing in the autumn as temperatures get colder. Levels then decline in the spring, once the animal has survived cold conditions over winter. In keeping with this, a recent study showed that injection of trehalose enhanced resistance to heat and cold stress and dehydration in the Antarctic midge (50). This physiological rise in levels of these cryoprotectants in winter is associated with induction of diapause, another mechanism specific to invertebrates that allows animals to survive harsh conditions. It is of interest in this context to note that inhibition of IIS pathways induced diapause in mosquitoes (24). Future studies will be necessary to determine the long-term effects of elevated circulating sugar levels on fly physiology and to determine whether conserved molecular and biochemical pathways, shared by insects and mammals, account for the abnormalities in sugar and fat homeostasis seen in *dilp* mutants.

Experimental Procedures

Generation of *dilp* Deletions. *dilp1–dilp5*, *dilp6*, and *dilp7* deletion lines were generated according to Parks et al. (35). Exelixis stock pairs were chosen with the deletion hunter tool (DrosDel Consortium). Parental lines were: d02657 and f05433 for *Df[dilp1–5]*; d01857 and f01395 for *Df[dilp6]*; and d00591 and f00251 for Df[dilp7]. For detailed crossing schemes, see *SI Experimental Procedures*.

Morphometry. The protocol of Brogiolo et al. (17) was used to quantify wing size, cell size, and cell number. For allometry experiments, wings were dis-

PHYSIOLOGY

sected in 70% ethanol and mounted in 4:5 lactic acid:ethanol. Genital arch posterior lobes were dissected in 70% ethanol, dehydrated in a series of 90% ethanol and 100% ethanol, and mounted in euparol. Slides were placed at approximately 55 °C to allow the euparol to harden. Wings were photographed using a 5× objective; genital arches using a 40× objective. Tissue areas were measured after outlining in ImageJ (National Institutes of Health).

Metabolic Assays. Phalloidin staining of fat body tissue was carried out according to manufacturers' protocols and (51). For lysotracker staining of live fat body tissue, 0.1 μM lysotracker Red DND-99 (Invitrogen) containing 10 μg/mL Hoechst 33342 (Invitrogen) was used (40). Metabolic rate was measured as the rate of heat production using a multicell differential scanning calorimeter (*SI Experimental Procedures*). Sugar levels in larval hemolymph were determined as described (26), under controlled conditions (*SI Experimental Procedures*). The experiment shown in Fig. 5*C* was done in a blind fashion: J.L. collected and coded hemolymph samples and H.Z. carried out the assay. Triglyceride levels in adult flies were determined according to (52).

ACKNOWLEDGMENTS. We thank J. Ewer for suggesting the deficiency approach; the *Drosophila* Genetic Resource Center of the Kyoto Institute of Technology, Japan, and the *Drosophila* Stock Collection at Harvard Medical School for providing fly stocks; A. Teleman for advice on triglyceride measurements; A. Shingleton and J. Shultz for advice on allometry measurements; and Jahda Hill for help with lysotracker assays. This work was supported by National Institutes of Health Grant R01 EY14290 (to L.P.) and the American Diabetes Association (to R.A.K. and L.P.).

1. Baserga R, Peruzzi F, Reiss K (2003) The IGF-1 receptor in cancer biology. *Int J Cancer* 107:873–877.
2. Kahn RC, et al. (2005) in *Joslin's Diabetes Mellitus*, *14th Edition*, eds Kahn RC, King GL, Moses AC, Weir GC, Jacobson AM, Smith RJ (Lippincott Williams & Wilkins, Boston, MA).
3. Nakae J, Kido Y, Accili D (2001) Tissue-specific insulin resistance in type 2 diabetes: Lessons from gene-targeted mice. *Ann Med* 33:22–27.
4. Taguchi A, White MF (2008) Insulin-like signaling, nutrient homeostasis, and life span. *Annu Rev Physiol* 70:191–212.
5. LeRoith D (2008) Clinical relevance of systemic and local IGF-I: Lessons from animal models. *Pediatr Endocrinol Rev 5 Suppl* 2:739–743.
6. Nandi A, Kitamura Y, Kahn CR, Accili D (2004) Mouse models of insulin resistance. *Physiol Rev* 84:623–647.
7. Leroith D, Accili D (2008) Mechanisms of disease: Using genetically altered mice to study concepts of type 2 diabetes. *Nat Clin Pract Endocrinol Metab* 4:164–172.
8. Duvillie B, et al. (1997) Phenotypic alterations in insulin-deficient mutant mice. *Proc Natl Acad Sci USA* 94:5137–5140.
9. Accili D, et al. (1996) Early neonatal death in mice homozygous for a null allele of the insulin receptor gene. *Nat Genet* 12:106–109.
10. Liu JP, Baker J, Perkins AS, Robertson EJ, Efstratiadis A (1993) Mice carrying null mutations of the genes encoding insulin-like growth factor I (Igf-1) and type 1 IGF receptor (Igf1r). *Cell* 75:59–72.
11. Louvi A, Accili D, Efstratiadis A (1997) Growth-promoting interaction of IGF-II with the insulin receptor during mouse embryonic development. *Dev Biol* 189:33–48.
12. Kido Y, Philippe N, Schaffer AA, Accili D (2000) Genetic modifiers of the insulin resistance phenotype in mice. *Diabetes* 49:589–596.
13. Doria, A (2005) in *Joslin's Diabetes Mellitus*, *14th Edition*, eds Kahn RC, King GL, Moses AC, Weir GC, Jacobson AM, Smith RJ (Lippincott Williams & Wilkins, Boston, MA).
14. Reijonen H, Cancannon P (2005) in *Joslin's Diabetes Mellitus*, *14th Edition*, eds Kahn RC, King GL, Moses AC, Weir GC, Jacobson AM, Smith RJ (Lippincott Williams & Wilkins, Boston, MA).
15. Petruzzelli L, Herrera R, Arenas-Garcia R, Fernandez R, Birnbaum MJ, Rosen OM (1986) Isolation of a *Drosophila* genomic sequence homologous to the kinase domain of the human insulin receptor and detection of the phosphorylated *Drosophila* receptor with an anti-peptide antibody. *Proc Natl Acad Sci USA* 83:4710–4714.
16. Fernandez-Almonacid R, Rosen OM (1987) Structure and ligand specificty of the *Drosophila melanogaster* insuln receptor. *Mol Cell Biol* 7:2718–2727.
17. Brogiolo W, Stocker H, Ikeya T, Rintelen F, Fernandez R, Hafen E (2001) An evolutionarily conserved function of the *Drosophila* insulin receptor and insulin-like peptides in growth control. *Curr Biol* 11:213–221.
18. Wu Q, Brown MR (2006) Signaling and function of insulin-like peptides in insects. *Annu Rev Entomol* 51:1–24.
19. Yang CH, Belawat P, Hafen E, Jan LY, Jan YN (2008) Drosophila egg-laying site selection as a system to study simple decision-making processes. *Science* 319:1679–1683.
20. Leevers, S. J (2001) Growth control: Invertebrate insulin surprises! *Curr Biol* 11:R209–212.
21. Riehle MA, Fan Y, Cao C, Brown MR (2006) Molecular characterization of insulin-like peptides in the yellow fever mosquito, Aedes aegypti: Expression, cellular localization, and phylogeny. *Peptides* 27:2547–2560.
22. Brown MR, et al. (2008) An insulin-like peptide regulates egg maturation and metabolism in the mosquito Aedes aegypti. *Proc Natl Acad Sci USA* 105:5716–5721.
23. Luckhart S, Riehle MA (2007) The insulin signaling cascade from nematodes to mammals: Insights into innate immunity of Anopheles mosquitoes to malaria parasite infection. *Dev Comp Immunol* 31:647–656.
24. Sim C, Denlinger DL (2008) Insulin signaling and FOXO regulate the overwintering diapause of the mosquito Culex pipiens. *Proc Natl Acad Sci USA* 105:6777–6781.
25. Cao C, Brown MR (2001) Localization of an insulin-like peptide in brains of two flies. *Cell Tissue Res* 304:317–321.
26. Rulifson EJ, Kim SK, Nusse R (2002) Ablation of insulin-producing neurons in flies: Growth and diabetic phenotypes. *Science* 296:1118–1120.
27. Ikeya T, Galic M, Belawat P, Nairz K, Hafen E (2002) Nutrient-dependent expression of insulin-like peptides from neuroendocrine cells in the CNS contributes to growth regulation in Drosophila. *Curr Biol* 12:1293–1300.
28. LaFever L, Drummond-Barbosa D (2005) Direct control of germline stem cell division and cyst growth by neural insulin in Drosophila. *Science* 309:1071–1073.
29. Broughton SJ, et al. (2005) Longer lifespan, altered metabolism, and stress resistance in Drosophila from ablation of cells making insulin-like ligands. *Proc Natl Acad Sci USA* 102:3105–3110.
30. Fernandez R, Tabarini D, Azpiazu N, Frasch M, Schlessinger J (1995) The *Drosophila* insulin receptor homolog: A gene essential for embryonic development encodes two receptor isoforms with different signaling potential. *EMBO J* 14:3373–3384.
31. Chen C, Jack J, Garofalo RS (1996) The *Drosophila* insulin receptor is required for normal growth. *Endocrin* 137:846–856.
32. Bohni R, et al. (1999) Autonomous control of cell and organ size by CHICO, a *Drosophila* homolog of vertebrate IRS1–4. *Cell* 97:865–875.
33. Stathopoulos A, Van Drenth M, Erives A, Markstein M, Levine M (2002) Whole-genome analysis of dorsal-ventral patterning in the Drosophila embryo. *Cell* 111:687–701.
34. Broughton S, et al. (2008) Reduction of DILP2 in Drosophila triages a metabolic phenotype from lifespan revealing redundancy and compensation among DILPs. *PLoS ONE* 3:e3721.
35. Parks AL, et al. (2004) Systematic generation of high-resolution deletion coverage of the Drosophila melanogaster genome. *Nat Genet* 36:288–292.
36. Hanai S, et al. (2004) Loss of poly(ADP-ribose) glycohydrolase causes progressive neurodegeneration in Drosophila melanogaster. *Proc Natl Acad Sci USA* 101:82–86.
37. Shingleton AW, Das J, Vinicius L, Stern DL (2005) The temporal requirements for insulin signaling during development in Drosophila. *PLoS Biol* 3:e289.
38. Shingleton AW, Frankino WA, Flatt T, Nijhout HF, Emlen DJ (2007) Size and shape: The developmental regulation of static allometry in insects. *Bioessays* 29:536–548.
39. Nation JL (2002) *Insect Physiology and Biochemistry* (CRC Press LLC, Boca Raton).
40. Scott RC, Schuldiner O, Neufeld TP (2004) Role and regulation of starvation-induced autophagy in the Drosophila fat body. *Dev Cell* 7:167–178.
41. Neufeld TP, Baehrecke EH (2008) Eating on the fly: Function and regulation of autophagy during cell growth, survival and death in Drosophila. *Autophagy* 4:557–562.
42. LeRoith D, Gavrilova O (2006) Mouse models created to study the pathophysiology of Type 2 diabetes. *Int J Biochem Cell Biol* 38:904–912.
43. LeRoith D, Lesniak M, Roth J (1981) Insulin in insects and annelids. *Diabetes* 30:70–76.
44. Eisenbarth, GS (2005) in *Joslin's Diabetes Mellitus*, *14th Edition*, eds Kahn RC, King GL, Moses AC, Weir GC, Jacobson AM, Smith RJ (Lippincott Williams & Wilkins, Boston, MA).
45. Taylor SI (1992) Lilly Lecture: Molecular mechanisms of insulin resistance. Lessons from patients with mutations in the insulin-receptor gene. *Diabetes* 41:1473–1490.
46. Kim SK, Rulifson EJ (2004) Conserved mechanisms of glucose sensing and regulation by Drosophila corpora cardiaca cells. *Nature* 431:316–320.
47. Wyatt GR, Kale GF (1957) The chemistry of insect hemolymph. II. Trehalose and other carbohydrates. *J Gen Physiol* 40:833–847.
48. Bale JS (2002) Insects and low temperatures: From molecular biology to distributions and abundance. *Philos Trans R Soc Lond B Biol Sci* 357:849–862.
49. Doucet D, Walker VK, Qin W (2009) The bugs that came in from the cold: Molecular adaptations to low temperatures in insects. *Cell Mol Life Sci* 66:1404–1408.
50. Benoit JB, Lopez-Martinez G, Elnitsky MA, Lee RE Jr, Denlinger DL (2009) Dehydration-induced cross tolerance of Belgica antarctica larvae to cold and heat is facilitated by trehalose accumulation. *Comp Biochem Physiol A Mol Integr Physiol* 152:518–523.
51. Hennig KM, Colombani J, Neufeld TP (2006) TOR coordinates bulk and targeted endocytosis in the Drosophila melanogaster fat body to regulate cell growth. *J Cell Biol* 173:963–974.
52. Teleman AA, Chen YW, Cohen SM (2005) 4E-BP functions as a metabolic brake used under stress conditions but not during normal growth. *Genes Dev* 19:1844–1888.